BMC Genomics

RESEARCH

Open Access

Comparative transcriptome, ultrastructure and histology analyses provide insights into the potential mechanism of growth arrest in south China carp (*Cyprinus carpio rubrofuscus*)

Zaixuan Zhong[1,2,3], Jiajia Fan[1,2,3], Yuanyuan Tian[1,2,3], Huaping Zhu[1,2,3*] and Dongmei Ma[1,2,3*]

Abstract

Background South China carp (*Cyprinus carpio rubrofuscus*), which is an economically important species, is traditionally cocultured with rice. Our previous study indicated that approximately 10–30% of these fish experienced growth arrest, severely impacting production. However, the molecular mechanism underlying growth inhibition in south China carp is currently unknown.

Results In this study, we compared the transcriptomes of the livers, muscles and intestines of carp in the fast-growing and slow-growing groups. We identified 2182, 2355 and 916 differentially expressed genes (DEGs), respectively. In the slow-growing group, the oxidative phosphorylation pathway was significantly upregulated in the liver. Transmission electron microscopy (TEM) confirmed mitochondrial damage in the liver, which was characterized by broken cristae and heterogeneous matrix. Additionally, analysis of antioxidant enzyme and transaminase activity also revealed that the livers in slow-growing individuals were unhealthy. In muscle tissue, the mitophagy and autophagy pathways were significantly dysregulated. Consequently, manifestations of mitochondrial damage and sparse myofilaments were clearly observed in slow-growing south China carp via TEM. Furthermore, pathways that regulate cell proliferation and migration, including the ECM receptor and focal adhesion, were significantly enriched in the intestine. Morphological examination revealed that the villus height and muscular layer height in the slow-growing group were significantly shorter than those in the fast-growing group, suggesting decreased intestinal cell motility. Overall, our study elucidated mitochondrial damage in the liver and muscle and detected morphological changes in intestinal villi.

Conclusions In summary, our results help elucidate the genetic architecture related to growth arrest in south China carp and provide a basis for further research on the growth of teleosts.

*Correspondence:
Huaping Zhu
zhhping2000@163.com
Dongmei Ma
mdm@prfri.ac.cn

Full list of author information is available at the end of the article

Keywords South China carp, Growth arrest, RNA-seq, Ultrastructure, Histology

Background

Growth-related traits have attracted significant attention within the aquaculture industry. Increasing the growth rate is a principal goal of selective breeding programs, as it directly influences productivity, costs, and economic returns [1]. Generally, the growth rate of fish is affected by environmental factors, genetic factors or a combination of these factors. Environmental factors, including temperature, stocking density, and nutrition, have been identified as common factors that impact growth rates [2–4]. In contrast, elucidating the genetic mechanisms that affect growth rate presents a formidable challenge, since the biological processes that regulate growth are complex and affected by multiple genes and signaling pathways [5, 6].

One of the common views about growth in fish species is that growth rates are predominantly controlled by growth hormone (GH) and insulin-like growth factors (IGFs), which regulate the synthesis and degradation of proteins and thereby control the rate of growth [7, 8]. Thanks to rapid and significant advances in sequencing technology, such as whole-genome sequencing (WGS), bulking seropositive analysis (BSA) and transcriptome analysis, an increasing number of growth-related genes have been identified in economically important fish [9, 10]. For example, the *pax3* and *six4* genes have been implicated in growth-related biological processes in grass carp (*Ctenopharyngodon idella*) [5]. A recent investigation in the leopard coral grouper (*Plectropomus leopardus*) identified *per2* and *acadvl* as candidate growth-related genes through a genome-wide association study (GWAS) and RNA-seq [6]. These researches demonstrated that unveiling the genetic basis of growth could provide valuable insights to improve the breeding and management of fish.

South China carp (*Cyprinus carpio rubrofuscus*), which is a subspecies of common carp, is extensively cultivated around southern China, and it is a valuable resource in the aquaculture industry [11]. South China carp is characterized by rapid growth, large size and robust adaptability, and it has become a pivotal aquatic genetic resource for the breeding of novel strains [12, 13]. Several researches have revealed the effects environmental factors on the growth rate of south China carp [14, 15]. Our previous study pointed out that the body weight, daily weight gain, net weight gain, and specific growth rate of juvenile south China carp were all maximized, when the stocking density of was 43.48 fish/m^2 [14]. Besides, the weight gain rate and specific growth rate of the juvenile south China carp exhibited an upward trend as the crude protein level of feed increased from 25 to 45% [15]. Through five generations of consecutive systematic breeding, we successfully selected a new strain of south China carp named "Ruyuan No. 1" (GS-01-002-2021), which is particularly well-suited for rice–fish coculture systems. However, in previous decades, the germplasm resources of south China carp have been subjected to degradation, resulting in morphological abnormalities and stunted growth [16]. Our previous research indicated that 10–30% of south China carp may experience growth arrest, leading to decreased production and income [17]. Despite these observations, research into the molecular mechanisms that regulate growth in common carp remains limited. In a fast-growing common carp strain (*Cyprinus carpio* L.), 2b-RAD technology revealed that *Tox*, *PLK2* and *CD163* drive growth performance during the second half of the grow-out period (8–17 months). However, RAD sequencing of 1425 juveniles did not identify any genome-wide significant quantitative trait loci (QTLs) in common carp [18]. To our knowledge, no preliminary research has yet explored the mechanisms that regulate growth processes in south China carp. Therefore, investigating the potential genetic basis of growth inhibition is essential to facilitate the selective breeding of south China carp.

In the present study, we conducted a comprehensive transcriptome analysis to compare the expression profiles of livers, skeletal muscles and intestines of fast-growing and slow-growing south China carp (Fig. 1). Additionally, we examined the ultrastructure of livers and muscles and compared the morphological differences in the intestines of the two groups. To further evaluate the hepatic health, we quantified antioxidant enzyme and transaminase activity. Our findings could increase the understanding of the genetic mechanism underlying growth arrest and offer valuable insights for further selective breeding of south China carp.

Results

Assessment of RNA-seq data quality

To obtain transcriptomic profiles of livers, muscles and intestines, 18 cDNA libraries were constructed for the fast-growing group and slow-growing group. A total of 118.19 Gb of clean data were generated after quality control, with a Q30>95.19%, indicating the high quality of the sequencing data (Table S1). A total of 19.60, 18.21, 19.73, 20.01, 19.96 and 20.69 Gb of clean data were obtained for CI (Intestine of slow-growing group), TI (Intestine of fast-growing group), CL (Liver of slow-growing group), TL (Liver of fast-growing group), CM (Muscle of slow-growing group) and TM (Muscle of fast-growing group), respectively (Table S1). All the clean

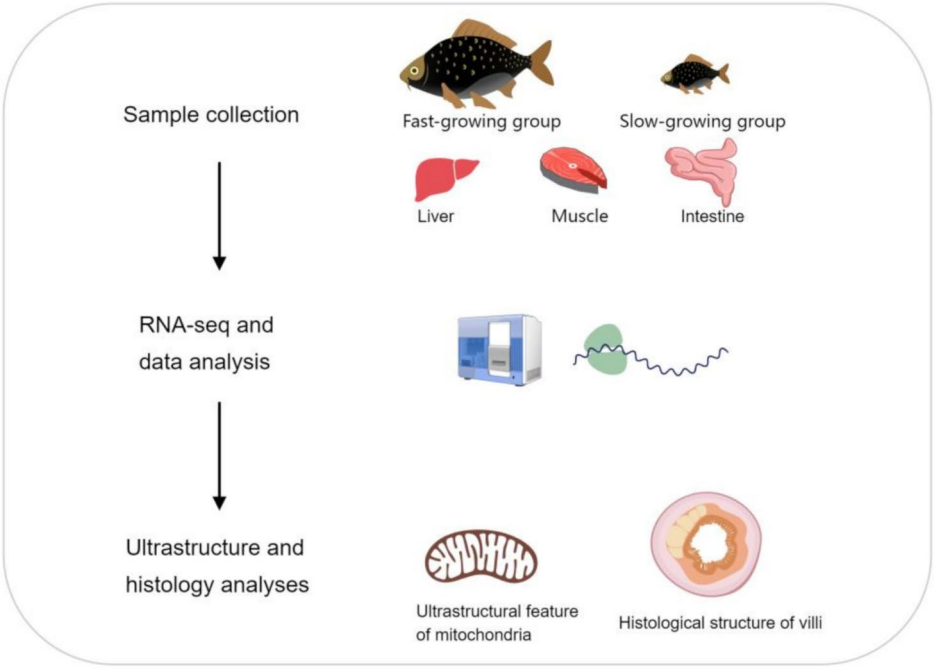

Fig. 1 The overall workflow of this research

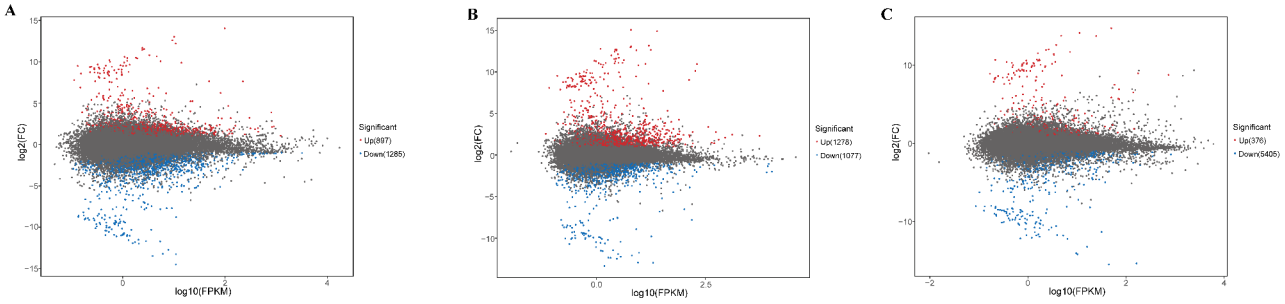

Fig. 2 MA plots of DEGs in liver (**A**, 897 up-regulated and 1,285 down-regulated), muscle (**B**, 1,278 up-regulated and 1,077 down-regulated) and intestine (**C**, 376 up-regulated and 540 down-regulated) between fast-growing and slow growing group. The red and blue dots represent up-regulated and down-regulated genes, respectively. Black dots represent genes with no significant expression difference

reads were mapped to the common carp genome, with mapping rates varying from 83.02 to 90.24%.

We subsequently conducted correlation analysis and principal component analysis (PCA) on the basis of the gene expression levels to evaluate the reliability of the samples (Fig. S1). The heatmap of Pearson's correlation between biological replicates indicated a strong correlation among samples (Fig. S1). The PCA results were consistent with those of the correlation analysis, suggesting high repeatability and consistency across the samples.

Differentially expressed gene (DEG) analysis

Three pairwise comparison groups (CL-TL, CM-TM and CI-TI) were established to identify DEGs in the livers, muscles and intestines, respectively. A total of 2182 DEGs (897 upregulated and 1285 downregulated), 2355 DEGs (1,278 upregulated and 1,077 downregulated), and 916 DEGs (376 upregulated and 540 downregulated) were identified in the CL-TL, CM-TM and CI-TI comparisons, respectively (Fig. 2). Three heatmaps were separately generated for the liver, muscle and intestine to visualize the DEGs between the fast-growing group and slow-growing group (Fig. S2). The transcriptomic profiles of each group were obviously different. Detailed information about the DEGs is summarized in Table S2.

Functional analysis by gene ontology (GO) enrichment and kyoto encyclopedia of genes and genomes (KEGG) pathway

All the DEGs were subjected to GO term and KEGG pathway analyses to explore their biological functions. In the GO functional enrichment analyses, similar GO

categories were identified for all three comparison groups (Fig. 3A, B and C). The most significantly enriched GO terms were "cellular process", "metabolic process" and "single-organism process" at the biological process (BP) level. With respect to the cellular component (CC) category, the DEGs were predominantly related to terms such as "cell", "cell part" and "organelle". In the molecular function (MF) category, the DEGs were associated mainly with the terms "binding" and "catalytic activity". Furthermore, we conducted a screening of GO terms to elucidate the specific biological pathways in which the DEGs were involved (Fig. 3D, E and F).

Notably, GO terms that were associated with mitochondrial function, such as "mitochondrial translational elongation" and "mitochondrial translational termination", were significantly enriched in CL-TL. Additionally, "mitochondrial gene expression" was also significantly enriched (Fig. 3D). For CM-TM, the GO term "mitochondrial RNA polymerase binding promoter specificity activity" was significantly enriched (Fig. 3E). Moreover, the term "extracellular matrix structural constituent" was significantly downregulated in CI-TI (Fig. 3F).

The top 20 most highly enriched KEGG pathways for the pairwise comparison groups are illustrated in Fig. 4. The results revealed that a total of five, nine and five pathways were significantly dysregulated in CL-TL (Fig. 4A), CM-TM (Fig. 4B) and CI-TI (Fig. 4C), respectively. The DEGs in the liver (CL-TL) were significantly enriched in oxidative phosphorylation (Fig. 4A), which could lead to mitochondrial dysfunction. Notably, the most significantly enriched pathway in muscle (CM-TM) was mitophagy, which is an indicator of a disrupted

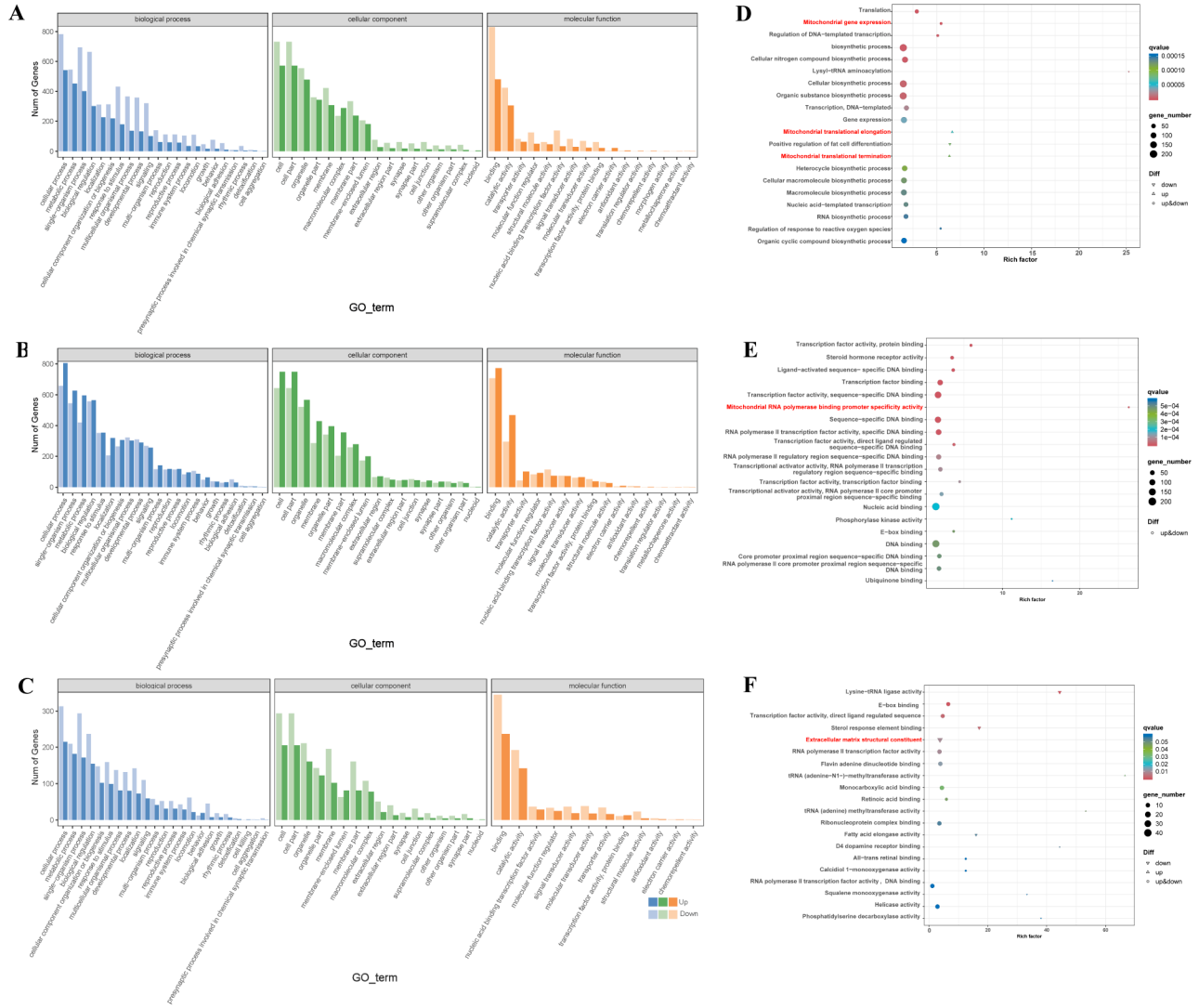

Fig. 3 GO classification and GO enrichment analysis of DEGs in liver (**A**), muscle (**B**) and intestine (**C**). DEGs were annotated at biological process (BP), cellular component (CC) and molecular function (MF) level. **D**, **E** and **F** represents GO enrichment pathways in liver, muscle and intestine, respectively

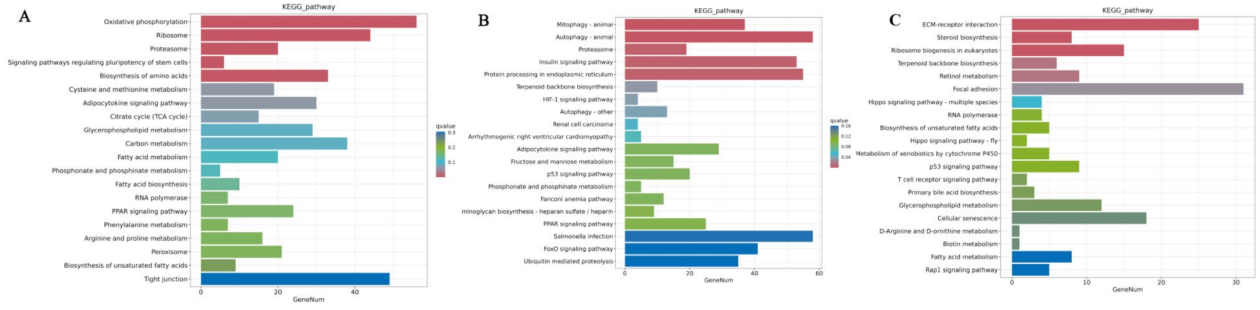

Fig. 4 Bar plots of top 20 enriched KEGG pathways of DEGs in liver (**A**), muscle (**B**) and intestine (**C**)

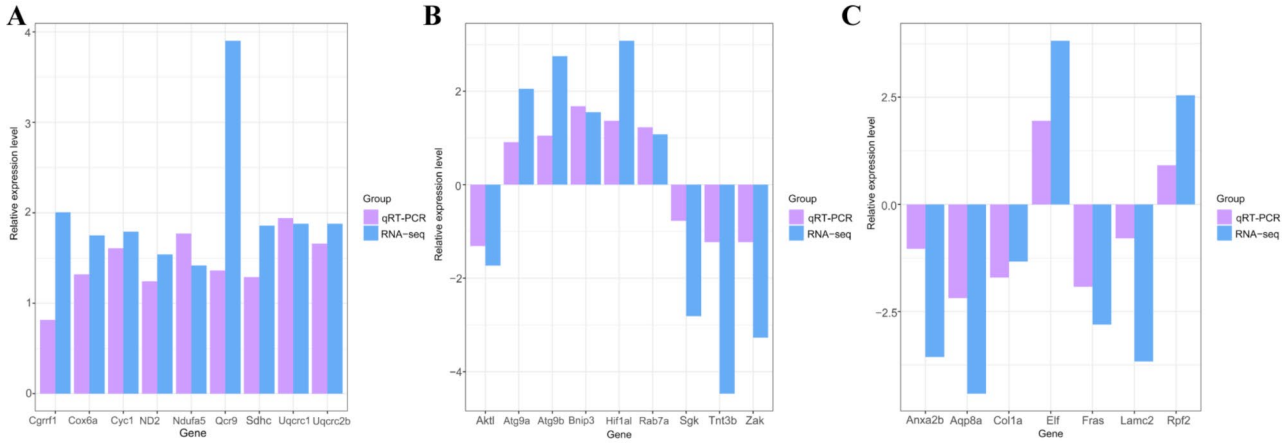

Fig. 5 Validation of DEGs by qRT-PCR to assess the reliability of RNA-seq. The results of qRT-PCR and RNA-seq were showed as purple and blue bars, respectively

mitochondrial network (Fig. 4B). Pathways related to cell proliferation and migration, such as ECM-receptor interaction and focal adhesion, were significantly enriched in the intestine (Fig. 4C).

DEGs involved in mitochondrial function and cell migration

To validate the accuracy of the transcriptome data, nine DEGs in the liver, nine DEGs in the muscle and seven DEGs in the intestine were selected, and their expression levels were verified by real-time quantitative PCR (qRT−PCR). The results indicated that the expression patterns of the DEGs were consistent between the qRT−PCR and RNA−Seq results (Fig. 5), validating the accuracy of the transcriptome sequencing data.

As demonstrated by the RNA-seq results, several genes and KEGG pathways that are associated with mitochondrial function were dysregulated in the liver and muscle of the slow-growing group. Interestingly, the oxidative phosphorylation (OXPHOS) pathway and all the DEGs (n=56) in this pathway were significantly upregulated in the liver (Fig. 6A). The expression of nine representative DEGs related to OXPHOS, namely, *Cox6a*, *Cyc1*, *Cgrrf1*, *ND2*, *Ndufa5*, *Qcr9*, *Sdhc*, *Uqcrc1*, *and Uqcrc2b*, is shown in Fig. 5A. *ND2* and *Ndufa5* encode the subunits of mitochondrial complex I; *Sdhc*, *Cox6a* and *Qcr9* encode the subunits of complex II; and *Cgrrf1*, *Cyc1*, *Uqcrc1* and *Uqcrc2b* encode the subunits of complex III. Furthermore, among the 37 mitophagy pathway-related genes that were differentially expressed in muscle, 27 genes were upregulated (Fig. 6B). The expression of four pro-apoptotic factors, namely, *bnip3*, *Atg9a*, *Atg9b* and *rab7*, was validated by qRT−PCR (Fig. 5B). Moreover, 19 genes that are involved in both the ECM-receptor interaction and focal adhesion pathways were downregulated in the intestine (Fig. 6C and D). As shown in Fig. 5C, *Lamc2* and *Col1a2*, which are the subunits of laminin and collagen, exhibited significantly decreased expression levels.

Ultrastructural features of mitochondria and histological structures of villi

In order to explore whether dysregulated pathway would affect the structure of tissues, we performed histological assay. Evident ultrastructural alterations in mitochondria were observed via transmission electron microscopy (TEM) in liver and muscle. The mitochondria from slow-growing individuals exhibited irregular cristae and relatively low-density, heterogeneous matrices. Conversely,

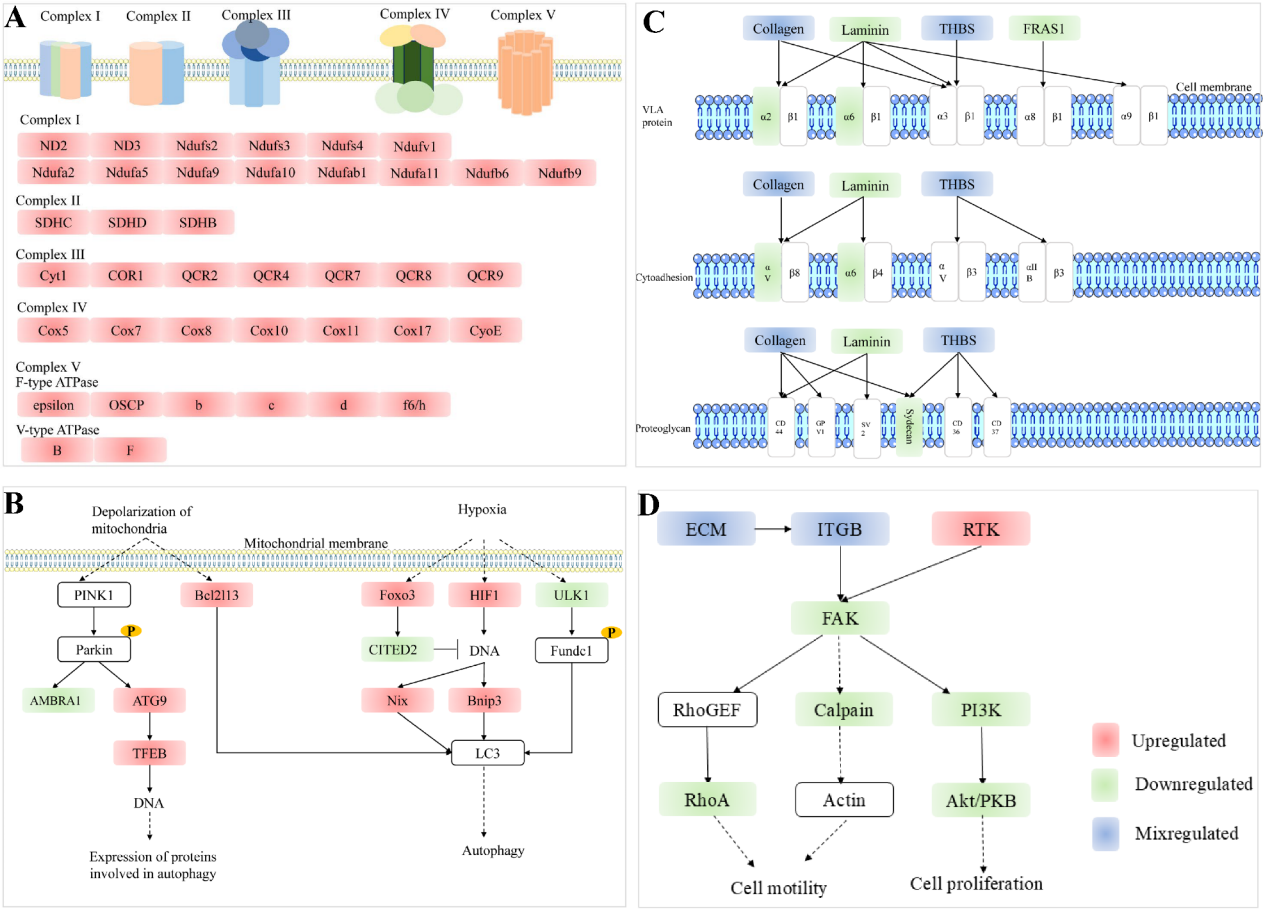

Fig. 6 The DEGs involved in oxidative phosphorylation (**A**), mitophagy (**B**), ECM-receptor interaction (**C**) and focal adhesion (**D**). The green boxes indicate down-regulated genes in slow-growing group compared with fast-growing group. The red boxes indicate up-regulated genes. The blue boxes indicated both down-regulated and up-regulated genes

the mitochondria from fast-growing individuals exhibited regular internal cristae, which appeared to be packed in a well-organized manner. In addition, the mitochondrial matrices of fast-growing individuals were homogeneous. (Fig. 7A and B). Similar damage to mitochondrial morphology was observed in muscle tissues (Fig. 7C and D). The myofilaments in the slow-growing group were loose and irregular, whereas those in the fast-growing group were tightly and neatly arranged.

In the slow-growing group, the villus height (VH) was significantly shorter than that in the fast-growing group, as presented in Table 1 (Fig. 7E and F, P=7.24E-22), whereas the villus width (VW) did not significantly differ between the two groups. Additionally, the muscular layer of the intestine was significantly thicker (P=4.02E-06) in the fast-growing group than in the slow-growing group.

Biochemical indices in the liver

To investigate health status of liver, we measured the activities of the total antioxidant capacity (TAOC) and superoxide dismutase (SOD). The results showed that TAOC and SOD were significantly lower in the slow-growing group than in the fast-growing group (3.03±0.25 U/ml vs. 2.19±0.19 U/ml, P=1.23E-12; 146.73±4.29 U/ml vs. 135.39±12.49 U/ml, P=1.19E-04; Fig. 8A and B). Concurrently, the levels of the aminotransferases alanine transaminase (ALT) and aspartate transaminase (AST) were significantly greater (P=1.83E-5 and P=8.28E-7, respectively) in slow-growing individuals (30.44±20.36 U/L vs. 77.37±33.10 U/L; 145.99±40.73 U/L vs. 282.62±84.36 U/L, respectively; Fig. 8C and D).

Discussion

Increasing the growth rate of economically important aquatic species has always been an important and challenging task. A deep understanding of the mechanisms underlying differences in growth rates can contribute to improving growth rates via more efficient breeding schemes [19]. It is well-documented that the molecular mechanisms associating with growth arrest vary among

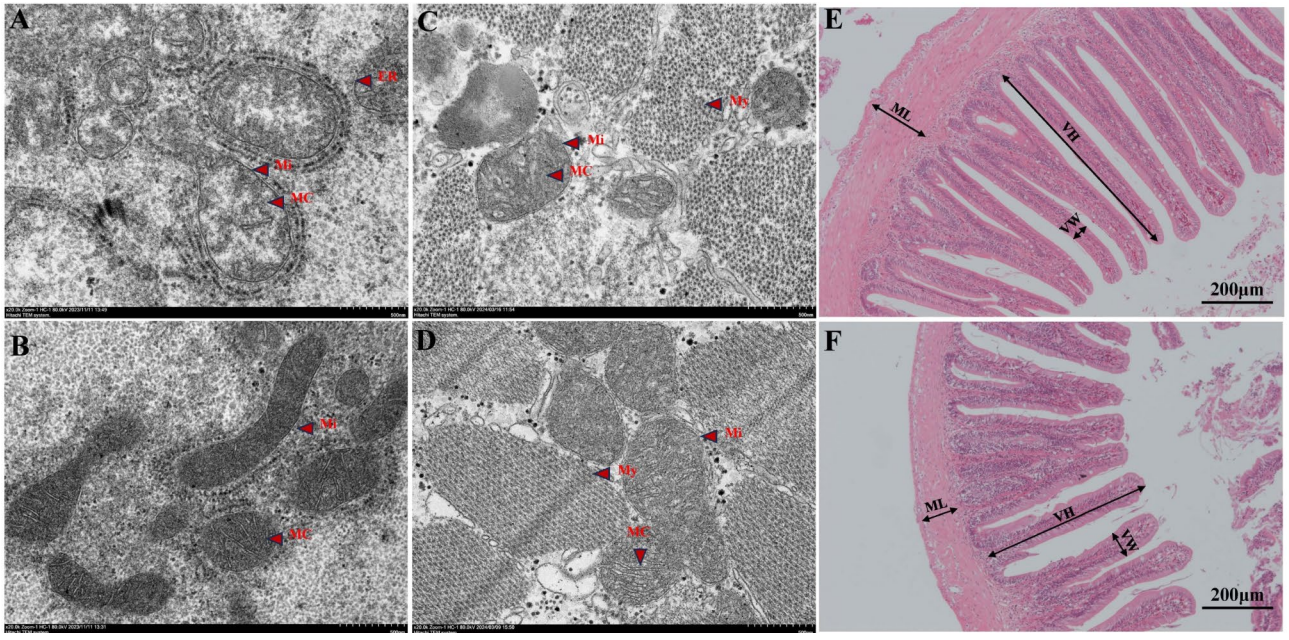

Fig. 7 Comparisons of the ultrastructural mitochondria in liver (**A**, **B**) and muscle (**C**, **D**) between fast-growing group and slow-growing group. The histological morphology of intestine (**E**, **F**). The scale represents 200 μm
ER: endoplasmic reticulum. Mi: mitochondria. MC: mitochondrial cristae. My: myofilament. VH: villi height. VW: villi width. ML: thickness of muscular layer

Table 1 Morphological traits of intestine in fast-growing and slow-growing Group

Group	Villus height (um)	Villus width (um)	Villus height/Villus width	Thickness of muscular layer (um)
FG	526.23 ± 80.97	101.58 ± 34.68	5.91 ± 2.35	95.59 ± 26.47
SG	316.94 ± 73.01	104.45 ± 27.67	3.24 ± 1.20	73.44 ± 12.91

different species [20, 21]. For example, a significantly lower expression level of GAPDH was detected in slow-growing grass carp [20]. In yellow perch (*Perca flavescens*), which has a relatively low growth rate, the staining density of alpha actinin, sarcoendoplasmic reticulum calcium ATPase, phosphoglucose isomerase 2, and creatine kinase was greater than that in fast-growing individuals [21]. To gain a better understanding of the molecular regulatory mechanisms underlying growth arrest in south China carp, we undertook transcriptional profiling analyses of liver, muscle and intestine from the fast-growing and slow-growing groups.

Impaired OXPHOS resulted in unhealthy liver

According to the KEGG analysis, the OXPHOS pathway was the most significantly dysregulated pathway in the liver tissues of the slow-growing group (Fig. 4A). As shown in Fig. 6A, several genes that encode components of five multiprotein complexes (I, II, III, IV and V) were significantly upregulated, suggesting dysregulation of the subunits that are involved in the OXPHOS system. The OXPHOS system, which is localized within the mitochondria, is responsible for generating approximately 90% of the total amount of cellular adenosine triphosphate (ATP) [22, 23]. Notably, half of the genes that encode subunits of cytochrome oxidase (COX) were upregulated. COX is the regulatory center of OXPHOS and prevents the accumulation of reactive oxygen species (ROS) [24]. Previous studies have pointed out that excessive byproducts of oxidative phosphorylation, such as ROS, can induce mitochondrial damage [25–27]. The TEM results revealed pronounced disorganization of the mitochondrial ultrastructure in the livers of the slow-growing group (Fig. 7A), confirming that upregulation of OXPHOS profoundly impacted mitochondrial morphology [28, 29] and impaired liver function. These results are consistent with previously reported results from rat studies, where impaired OXPHOS in hepatic mitochondria resulted in retarded growth [30].

The liver serves as the principal metabolic organ in fish, and its health is crucial for growth performance, as demonstrated in largemouth bass (*Micropterus salmoides*) and African catfish (*Clarias gariepinus*) [31, 32]. Under homeostatic physiological conditions, antioxidant enzymes such as SOD and TAOC modulate the equilibrium of ROS, thereby helping maintain the health of cells [33]. Our assessment of antioxidant enzyme activity revealed that the TAOC and SOD activities were significantly lower in slow-growing south China carp (Fig. 8A and B). Since the OXPHOS level increased as the

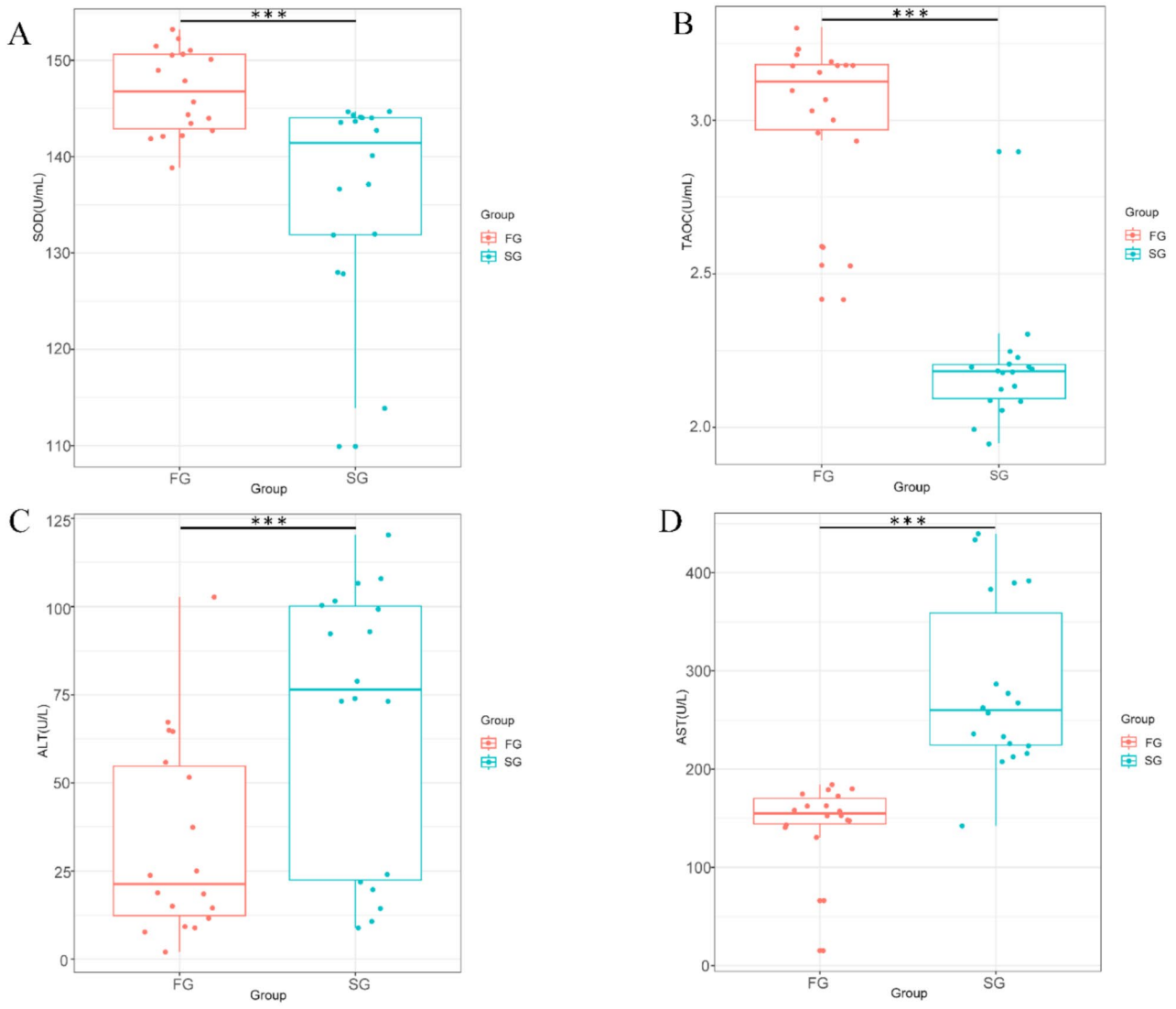

Fig. 8 Comparison of activity of SOD (**A**), TAOC (**B**), ALT (**C**) and AST (**D**) in liver tissue. FG and SG represents fast-growing group and slow-growing group. respectively. * $P < 0.05$, ** $P < 0.01$, *** $P < 0.001$

antioxidant enzyme activity decreased, we hypothesized that the livers in this group were unhealthy. ALT and AST are two important enzymes that reflect the health condition of the liver [34, 35]. Our ELISA results revealed a significant increase in the ALT and AST activities in the slow-growing group (Fig. 8C and D), which was consistent with the evidence of hepatic damage. Therefore, hepatic impairment may be one reason that explains growth inhibition.

Mitophagy and autophagy hampered the muscle development

Skeletal muscle, which constitutes 50–70% of body weight, is a critical determinant in aquaculture, and it directly influences the quantity and quality of meat [20, 36]. Consequently, elucidating the genetic factors and molecular mechanisms that regulate skeletal muscle development is crucial and essential for increasing meat yields [37]. Given the complexity of muscle growth, the genetic determinants that are implicated in this process vary across different fish species [20, 21]. For example, the GH/IGF axis was significantly enriched in muscle tissues, with *Igfbp1* downregulated and *Ghr2* upregulated in slow-growing grass carp [20]. Proteomic profiling of skeletal muscles from yellow perch (*Perca flavescens*) revealed that growth was associated not only with metabolic enzymes but also with myoD and myogenin [21]. In the present study, our analysis revealed significant enrichment of the mitophagy pathway, characterized by the upregulation of the mitophagy receptors Bnip3 and Bcl2 (Fig. 6B). Accordingly, the ultrastructural features of the mitochondria included irregular cristae and swelling,

indicating mitochondrial damage. The mitochondria in muscle participate in metabolic regulation and ATP production, which are two key elements of muscle contractibility and plasticity. Mitochondrial dysfunction such as mitophagy can impair energy metabolism by disrupting the balance between ATP production and consumption, which may hamper the development of muscle [38]. It has been reported in Nile Tilapia (*Oreochromis niloticus*) that genes involved in mitophagy showed upregulation in atrophying muscle [39]. Generally, mitophagy could be induced by cellular stress and disease. A recent study in zebrafish demonstrated that fasting could induce mitophagy in muscle [40]. Our previous study (unpublished data) found that the expression level of the *Orexin* gene was lower and that the frequency of food intake was significantly lower in the slow-growing group than in the fast-growing group. Consequently, we inferred that slow-growing individuals may experience a loss of appetite and starvation, which is likely to lead to mitophagy.

In addition, autophagy was also dysregulated in slow-growing south China carp. The expression level of the *Barkor* gene, which encodes a protein that is specifically associated with autophagosomes and is crucial for the autophagy process [41], was significantly increased in the slow-growing group. Autophagy, which is a vital catabolic process, is essential for maintaining cellular metabolism and energy homeostasis [42]. In teleost fish, impaired autophagy has been implicated in skeletal muscle atrophy and other severe skeletal muscle myopathies [43]. In this study, the TEM results revealed tightly and neatly arranged myofilaments in the fast-growing group (Fig. 7D). In contrast, loose and irregularly arranged myofilaments were observed in the slow-growing group (Fig. 7C), suggesting autophagy may influence the muscle development in south China carp.

Our findings on the mitochondrial damage in the liver and muscle tissues of slow-growing carp suggested that nutritional management strategies should pay attention to mitochondrial health. It has been reported that microbial feed additives (including pre-, pro-, and synbiotics) showed promising effects in terms of affecting antioxidant enzymes activities in fish [44]. Besides, nucleotide enriched diets could regulate the mitochondrial enzyme activity, antioxidant status and enhance the growth of *Sparus aurata* [45]. Therefore, we could take measures involving the use of dietary supplements such as antioxidants and feed additives to protect mitochondrial function of south China carp.

The histological morphology of intestine changed

The intestine is a multifunctional tissue that plays an important role in the processes of feed digestion, nutrient absorption, and modulation of the gut microbiota [46, 47]. The morphological integrity and health of the intestine are pivotal for influencing nutrient assimilation, which subsequently impacts growth performance [48, 49]. In *Megalobrama amblycephala*, comparative intestinal transcriptomic analysis revealed that PI3K-Akt/NF-κB/TCR inflammatory signaling pathway activation may lead to growth inhibition [50]. In our study, the focal adhesion and ECM pathways were significantly dysregulated in the slow-growing group (Fig. 4C). Focal adhesion is a form of intracellular junction that connects the ECM to the intracellular cytoskeleton in polarized epithelial cells, such as epithelial cells in the intestine. A major function of focal adhesion signaling is to direct the migration of epithelial cells in the intestinal villi [51]. Therefore, we hypothesized that the structure or morphology of the intestinal villi may be affected.

Histological assessment via HE staining revealed pronounced changes in the intestines of the slow-growing group (Fig. 7E and F), including considerably thinner muscular layers and shorter VHs. Evaluating the histological structure of digestive organs, such as the intestine, provides valuable information about health status and digestive capacity. Interestingly, it has been well documented that a decreased VH is correlated with a slow growth rate in fish, such as in orange-spotted grouper (*Epinephelus coioides*) and Nile tilapia [52, 53]. Thus, the results of present study were consistent with those of previous studies, suggesting that a decreased VH could adversely influence the digestive and absorptive functions of south China carp, thereby impacting their growth rate. These findings reminded us to take the health of gut into account during the breeding of south China carp. Several studies have pointed out that supplementation of prebiotics in fish improves intestinal health and increases villus length [54, 55], which may provide clues for the prevention of growth arrest in south China carp.

Conclusion

In summary, we elucidated the molecular pathways and specific genes associated with growth arrest in south China carp. The results indicated that mitochondrial dysfunction and the inhibition of villus cell proliferation are key factors that influence the growth rate of south China carp. These hypotheses were substantiated by both TEM and histological analyses, which provide evidence of the observed inhibition of growth at the cellular and tissue levels. Our comprehensive findings could provide a genetic basis for selective breeding of fast-growing south China carp, which is essential for improving the efficiency of farming. However, further functional research is needed to explore the regulatory roles of key DEGs genes to gain a deeper understanding of their functions.

Methods

Experimental design and sample collection

The south China carp used in our study were collected from Gudou Aquatic Co., Ltd., Jiangmen, China. A full-sib family was constructed using two three-year-old parents in 2021. About 2000 fries were randomly chosen and placed in the same pond. The fish were fed a commercial diet (Guangfo Feed Co. Ltd., Foshan, China) twice a day (8:00 AM and 5:00 PM) until satiated for six months. Subsequently, approximately 500 individuals were randomly selected for trait measurement including body weight and body length. Individuals in the top 5% in terms of body weight (n=25, 536.39±75.18 g) were considered the fast-growing group, whereas individuals in the bottom 5% in terms of body weight (n=25, 11.35±3.78 g) were considered the slow-growing group. The fish were fasted for 24 h before sample collection and anesthetized with 100 mg/L MS-222 (Sigma, USA). Nine fish from each group were randomly selected for liver, muscle and intestine harvesting, and these tissues were immediately placed in liquid nitrogen and stored at -80 °C. The blood of each individual was drawn with a 2-mL syringe and centrifuged for 8 min at 4 °C. The serum was retained and stored at -80 °C for further enzyme activity tests.

RNA extraction, library construction, and sequencing

The liver, muscle and intestine were collected from nine fish in the fast-growing group and nine fish in the slow-growing group for RNA-seq. Three samples from each group were mixed and considered one replicate for RNA isolation. Total RNA was extracted with a HiPure Unviersal RNA Mini Kit (Magen, Guangzhou, China) according to the manufacturer's instructions.

The purity and concentration of total RNA were assessed with a NanoDrop 2000 spectrophotometer. An Agilent 2100 bioanalyzer was used to assess the integrity of the RNA. Subsequently, eighteen cDNA libraries were constructed with the TruSeq RNA Sample Prep Kit v2 (Illumina, San Diego, CA, United States). The libraires were named CL1, CL2, and CL3 (liver of the fast-growing group); TL1, TL2, and TL3 (liver of the slow-growing group); CM1, CM2, and CM3 (muscle of the fast-growing group); TM1, TM2, and TM3 (muscle of the slow-growing group); CI1, CI2, and CI3 (intestine of the fast-growing group); and TI1, TI2, and TI3 (intestine of the slow-growing group). All the cDNA libraries were sequenced on an Illumina NovaSeq 6000 platform, generating 150 bp paired-end reads.

DEGs and enrichment analysis

The quality of the raw data was evaluated with fastp [56]. Low-quality reads and adaptors were removed with Trimmomatic 0.39 [57]. The RNA-seq data of liver was the same one used in our previous study [58]. The clean reads were subsequently mapped to the reference genome (Cyprinus_carpio_carpio. Cypcar_WagV4.0.108.genome.fa) via HISAT2 v2.2.0 [59]. Stringtie v2.2.0 was used to assemble the RNA-Seq alignments into potential transcripts [60]. PCA was conducted to evaluate the dispersion of the samples. The DESeq 2 package was used to identify the DEGs [61]. Genes with a |log2fold change| ≥ 1 and adjusted p<0.05 were considered DEGs. GO enrichment and KEGG pathway enrichment analyses were performed with clusterProfiler 4.0 [62].

DEG validation by qRT–PCR

To verify the accuracy of the RNA-seq data, a total of 25 DEGs (9, 9 and 7 from the liver, muscle and intestine samples, respectively) were selected for qRT−PCR. All the primers that were used for qRT−PCR were designed with Primer Premier 5 and are listed in Table 2. The total RNA from each replicate was reverse transcribed into cDNA with the PrimeScript RT Reagent Kit with gDNA Eraser (Takara, Dalian, China). The qRT−PCR was performed in 20 μl (2×SYBR Green qRT−PCR Premix: 10 μl, forward primer: 0.4 μl, reverse primer: 0.4 μl, cDNA: 1 μl, and nuclease-free water: 8.2 μl) on a 7500 Real-Time PCR System (Applied Biosystems, Foster City, CA, USA) under the following conditions: 95 °C for 30 s, followed by 35 cycles of 95 °C for 10 s, 60 °C for 10 s and 72 °C for 30 s. To ensure reproducibility, qRT-PCR reactions for each sample were performed in three technical replicates and three biological replicates. The relative gene expression levels were determined via the $2^{-\Delta\Delta Ct}$ method, with β-actin used as the reference gene.

Histological assay and intestinal villus measurement

The intestines of fast-growing carp (n=6) and slow-growing carp (n=6) were collected and fixed with 4% paraformaldehyde solution for histological analysis. After dehydrating with gradient alcohol and clearing with xylene, samples were wax-soaked and sliced on the paraffin slicer. The 5 μm sections were routinely stained with hematoxylin and eosin (H&E), after dewaxing and dehydrating with xylene and ethanol. The VH and VW of ten villi and ten muscular layers in each section were measured by ImageJ 1.51 software, the difference between two groups were analyzed.

TEM observation

Fresh liver, muscle and intestine samples from the fast-growing group (n=3) and slow-growing group (n=3) were collected and cut into 1-mm^3 cubes. All the samples were fixed in a 2.5% glutaraldehyde solution for 2 h, washed three times with 0.1 M PBS, fixed with 2% osmium tetroxide, washed three times with 0.1 M PBS, dehydrated in an acetone dilution series and embedded in Epon resin. Ultrathin Sects. (50–80 nm) were

Table 2 Primers used in the study

Gene name	Primer name	Sequence (5′-3′)	Tm	Product length
Cox6a	cox_f	CCTCAGGGCTCAACAACACC	60	179
	cox_r	GTAGAGCTCCTTACAGCGTTCACT		
Cyc1	cyc1_f	TCTGTACTTTCCTGAGGTGGGC	60	186
	cyc1_r	AGGCAGCAGTTTGGCTTTATTT		
ND2	nd2_f	TTATCATAACCTCCGCAGCATT	60	233
	nd2_r	GGCGGTTAGGGCTATGGC		
Cgrrf1	cgr_f	GGAGCCACAGCCCGAAAG	60	163
	cgr_r	GCACACACAGCCGTCACATAC		
Ndufa5	ndu_f	CCTACAGGAAATACACCGAGCA	60	203
	ndu_r	GTTCGCTGGTGCGTCCTC		
Qcr9	qc_f	GGCTGGAGAAGCGGTATTTG	60	144
	qc_r	CCATCCAGCAGGGTCACATC		
Sdhc	sd_f	GGCTTTCCCAGTGGCTTACC	60	199
	sd_r	TGTCTTCTTGATTTGTGCGTCTC		
Uqcrc1	uq1_f	AGGCACAAAGAAGCACCCAC	60	287
	uq1_r	TACCCTGGAAGGCAGTAGCAT		
Uqcrc2b	uq2_f	GTCGTGGCGAGCGAAAGT	60	166
	uq2_r	CAGACGCATCGAAGGGTTG		
Aktl	akt_f	TGTGGACGACTGCCCTTCTAC	60	217
	akt_r	CGTCCTCCCAGTGAATACCG		
Atg9a	atg9a_f	GGGTAATGCCCACCGCTAT	60	202
	atg9a_r	AGAGCAAGTATCACCCACACCA		
Atg9b	atg9b_f	GGACGCTCAGACAGGACCAT	60	196
	atg9b_r	GGCAGCAGAAGCCGCAC		
Bnip3	bnip_f	AATCAGAGCCGTTCTCATCGA	60	222
	bnip_r	GAGTGCTGCCACCTCCATTAT		
Hif1al	hif_f	AGGCACTGGCTGGCTTCA	60	170
	hif_r	TGTGGCAAGGATGTCTCGTAAT		
Rab7a	rab_f	TAACAACCAAGCGGGCACA	60	207
	rab_r	CTGCTGATGGCTTGGCTCTAT		
Sgk	sgk_f	GGACGGTGGACTGGTGGTG	60	165
	sgk_r	GGCCCTCCAGCAGGTGTC		
Tnt3b	tnt3b_f	ACAAGGAGCGTCAGGCAAGA	60	177
	tnt4b_r	TTTCAGTTTGCTTCTTACCTCCC		
Zak	zak_f	CAATGGACATCGCTAAAGGCA	60	152
	zak_r	GGTGTGGGAATGAAACTTGGAC		
Anxa2b	anx_f	GACAAAACGCAGTTGCTCACA	60	190
	anx_r	AGTGCCCAGACCCTTCATAGAT		
Aqp8a	aqp_f	TTGTGCGTTTACCTTATCGGAG	60	268
	aqp_r	CCAGATGACTTCGGGTCCTTA		
Col1a	col_f	AAGAAGAACCCTGCCCGTACT	60	226
	col_r	TCTCGCCGAACCAAATGTG		
Elf	elf_f	ATGACCTTCGGCAGTAACACC	60	138
	elf_r	ATTCAGCAGCCTGGCATCA		
Fras	fras_f	GTCTTCCGTCCGTTGTTTCAC	60	280
	fras_r	TTCAATCGTAGGAGCATCTTCATC		
Lamc	lamc_f	AAGCCATAGACCTCATCCGC	60	277
	lamc_r	CCCTCCACCATACCCTTCAG		
Rpf2	rpf_f	CGTACAGACTTACACGATGGCAC	60	204
	rpf_r	TAGAGCACAGCGTTGGGTTTC		

double-stained with 2% uranyl acetate and lead citrate and examined with a transmission electron microscope (Hitachi HT7800, 80 kV). Three visual fields from each section were observed. Images were captured with a Hitachi TEM system.

Determination of antioxidant enzyme activity and transaminase activity

The serum and liver tissues from 18 fast-growing individuals and 18 slow-growing individuals were analyzed to assess their antioxidant activity and liver function. The activities of antioxidant enzymes, including TAOC and SOD, in the serum and liver were measured with kits following the manufacturer's standard protocols (Nanjing Jiancheng Bioengineering Inc., Nanjing, China). The enzyme activities of ALT and AST in the serum were examined with commercial kits (Nanjing Jiancheng Bioengineering Inc., Nanjing, China) to assess liver function.

Statistical analysis

The qRT–PCR result, villus measurement and activity of enzyme, were analyzed by *t*-tests in R-4.3.0 software (https://www.r-project.org/). All data were subjected to normality and homoscedasticity testing. The experimental results are presented as mean ± standard deviation (SD). $P < 0.05$, $P < 0.01$ and $P < 0.001$ represented significant difference, highly significant difference and extremely significant difference between different groups, respectively.

Abbreviations

DEG	Differentially expressed gene
TEM	Transmission electron microscopy
WGS	Whole genome sequencing
BSA	Bulked Sergeant Analysis
GWAS	Genome-wide association study
QTL	Quantitative trait locus
PCA	Principal component analysis
OXHPO	The oxidative phosphorylation
ATP	Adenosine triphosphate
COX	Cytochrome oxidase
ROS	Reactive oxygen species
SOD	Superoxide dismutase
TAOC	Total antioxidant capacity
ALT	Alanine transaminase
AST	Aspartate transaminase

Supplementary Information

The online version contains supplementary material available at https://doi.org/10.1186/s12864-024-11081-9.

Supplementary Figure S1: The principal component analysis (**A**) and heatmap of correlations between fast-growing and slow-growing group (**B**). **Supplementary Figure S2**: The heatmap of DEGs. Red and blue indicates up-regulated and down-regulated genes, respectively. (**A**) DEGs in liver. (**B**) DEGs in muscle. (**C**) DEGs in intestine. **Supplementary Table S1**: Summary of transcriptome sequencing data Statistics

Supplementary Table S2: Information of DEGs identified in liver, muscle and intestine, respectively

Author contributions

ZX, HP and DM conceived and designed the study. ZX, JJ and YY conducted the experiment and analyzed the data. ZX and DM wrote the manuscript. HP reviewed and edited the manuscript.

Funding

This work was supported by the National Key Research and Development Program of China (2023YFD2400203), Guangdong Basic and Applied Basic Research Foundation (2024A1515013143), the National Natural Science Foundation of China (32072971), Guangdong Basic and Applied Basic Research Foundation (2023A1515110020), Central Public-interest Scientific Institution Basal Research Fund, CAFS (2023SJHX4), the Seed Industry Revitalization Project of the Guangdong Provincial Special Fund for Rural Revitalization Strategy (2022-SPY-00-019), the Guangdong Provincial Special Fund for Modern Agriculture Industry Technology Innovation Teams (2023KJ150) and Central Public-interest Scientific Institution Basal Research Fund, CAFS (2023TD37).

Data availability

The raw sequencing reads of this study have been deposited in National Genomics Data Center (https://ngdc.cncb.ac.cn/gsa/) with GSA accession number CRA018298.

Declarations

Ethics approval and consent to participate

All experiments were approved by the Laboratory Animal Ethics Committee of Pearl River Fisheries Research Institute, CAFS and were performed following the guidelines for the care and use of laboratory animals.

Consent for publication

Not applicable.

Competing interests

The authors declare no competing interests.

Author details

[1]Pearl River Fisheries Research Institute, Chinese Academy of Fishery Sciences, Guangzhou, Guangdong, China
[2]Key Laboratory of Tropical and Subtropical Fishery Resources Application and Cultivation, Ministry of Agriculture and Rural Affairs, Guangzhou, Guangdong, China
[3]Guangdong Provincial Key Laboratory of Aquatic Animal Immunology and Sustainable Aquaculture, Guangzhou, Guangdong, China

Received: 14 August 2024 / Accepted: 21 November 2024
Published online: 02 December 2024

References

1. Føre M, Frank K, Norton T, Svendsen E, Alfredsen JA, Dempster T, Eguiraun H, Watson W, Stahl A, Sunde LM. Precision fish farming: a new framework to improve production in aquaculture. Biosyst Eng. 2018;173:176–93.
2. Hoseini SM, Yousefi M, Hoseinifar SH, Van Doan H. Effects of dietary arginine supplementation on growth, biochemical, and immunological responses of common carp (*Cyprinus carpio* L.), stressed by stocking density. Aquaculture. 2019;503:452–9.
3. Wang Q, Xu Z, Ai Q. Arginine metabolism and its functions in growth, nutrient utilization, and immunonutrition of fish. Anim Nutr. 2021;7(3):716–27.
4. Volkoff H, Rønnestad I. Effects of temperature on feeding and digestive processes in fish. Temperature. 2020;7(4):307–20.
5. Triantaphyllopoulos KA, Cartas D, Miliou H. Factors influencing GH and IGF-I gene expression on growth in teleost fish: how can aquaculture industry benefit? Rev Aquacult. 2020;12(3):1637–62.
6. Reindl KM, Sheridan MA. Peripheral regulation of the growth hormone-insulin-like growth factor system in fish and other vertebrates. Comp Biochem Phys A. 2012;163(3–4):231–45.
7. Yue G, Wang L. Current status of genome sequencing and its applications in aquaculture. Aquaculture. 2017;468:337–47.

8. Luo L, Huang R, Zhang A, Yang C, Chen L, Zhu D, Li Y, He L, Liao L, Zhu Z. Selection of growth-related genes and dominant genotypes in transgenic Yellow River carp *Cyprinus carpio* L. Funct Integr Genomic. 2018;18:425–37.
9. Hao Y, Jia X, Yuan L, Liu Y, Gui L, Shen Y, Li J, Xu X. Genome-wide association study reveals growth-related SNPs and candidate genes in grass carp (*Ctenopharyngodon idella*). Aquaculture. 2023;577:739979.
10. Wang T, Wu X, Song L, Yang Y, Gong S, Zeng L, Tao Y, Zhong C, Meng Z, Liu X. Identification of candidate growth-related SNPs and genes using GWAS and transcriptome analyses in leopard coral grouper (*Plectropomus leopardus*). Aquaculture. 2023;574:739677.
11. Wu X. Monographs of Cyprinidae in China II. Shanghai: Shanghai People's; 1977.
12. Ma D, Huang Z, Zhu H, Xie J. Morphological characteristics and genetic analysis of the rice flower carp in the northern region of Guangdong Province. Prog Fish Sci. 2019;40(2):33–42.
13. Zhong Z, Fan J, Su H, Li Y, Ma D, Zhu H. Genetic sources and diversity of the paddy field carp in the Pearl River basin inferred from two mitochondrial loci. Front Ecol Evol. 2022;10:896609.
14. Li P, Ma D, Zhu H, Wen T. Effects of stocking density on growth traits of juvenile *Cyprinus carpio Rubrofuscus*. J Fisheries Res. 2019;41(1):63–9.
15. Xie Y, Chen X, Huang W, Cao J, Wu H, Wang G. Effects of protein level on growth, body composition and serum biochemical indices of Chinese ink carp *Procypris Merus*. Fisheries Sci. 2023;42(5):847–53.
16. Zhu H, Su H, Ma D, Huang Z. Comparative analysis of genetic diversity in *Cyprinus carpio rubrofuscus* among selective-breeding population and landraces. J Agr Biotech. 2018;26:1371–81.
17. Chen S, Ma D, Zhong Z, Fan J, Zhu H, Su H. Growth performance, feed intake and vegf121 gene expression feature of dwarf *Cyprinus carpio Rubrofuscus*. Prog Fish Sci. 2024;45:1–12.
18. Palaiokostas C, Kocour M, Prchal M, Houston RD. Accuracy of genomic evaluations of juvenile growth rate in common carp (*Cyprinus carpio*) using genotyping by sequencing. Front Genet. 2018;9:350926.
19. Robledo D, Rubiolo JA, Cabaleiro S, Martínez P, Bouza C. Differential gene expression and SNP association between fast-and slow-growing turbot (*Scophthalmus maximus*). Sci Rep-UK. 2017;7(1):12105.
20. Lu X, Chen HM, Qian XQ, Gui JF. Transcriptome analysis of grass carp (*Ctenopharyngodon idella*) between fast-and slow-growing fish. Comp Biochem Phys D. 2020;35:100688.
21. Kwasek K, Choi YM, Wang H, Lee K, Reddish JM, Wick M. Proteomic profile and morphological characteristics of skeletal muscle from the fast-and slow-growing yellow perch (*Perca flavescens*). Sci Rep-UK. 2021;11(1):16272.
22. Elbassiouny AA, Lovejoy NR, Chang BS. Convergent patterns of evolution of mitochondrial oxidative phosphorylation (OXPHOS) genes in electric fishes. Philos T R Soc B. 2020;375(1790):20190179.
23. Fernandez-Vizarra E, Zeviani M. Mitochondrial disorders of the OXPHOS system. FEBS Lett. 2021;595(8):1062–106.
24. Kadenbach B. Complex IV–the regulatory center of mitochondrial oxidative phosphorylation. Mitochondrion. 2021;58:296–302.
25. Nesci S, Trombetti F, Pagliarani A, Ventrella V, Algieri C, Tioli G, Lenaz G. Molecular and supramolecular structure of the mitochondrial oxidative phosphorylation system: implications for pathology. Life. 2021;11(3):242.
26. Hernansanz-Agustín P, Enríquez JA. Generation of reactive oxygen species by mitochondria. Antioxidants. 2021;10(3):415.
27. Belhadj Slimen I, Najar T, Ghram A, Dabbebi H, Ben Mrad M, Abdrabbah M. Reactive oxygen species, heat stress and oxidative-induced mitochondrial damage. A review. Int J Hyperther. 2014;30(7):513–23.
28. Sun Z, Lan X, Ahsan A, Xi Y, Liu S, Zhang Z, Chu P, Song Y, Piao F, Peng J. Phosphocreatine protects against LPS-induced human umbilical vein endothelial cell apoptosis by regulating mitochondrial oxidative phosphorylation. Apoptosis. 2016;21:283–97.
29. Herbers E, Kekäläinen NJ, Hangas A, Pohjoismäki JL, Goffart S. Tissue specific differences in mitochondrial DNA maintenance and expression. Mitochondrion. 2019;44:85–92.
30. Peterside IE, Selak MA, Simmons RA. Impaired oxidative phosphorylation in hepatic mitochondria in growth-retarded rats. Am J Physiol-Endoc M. 2003;285(6):E1258–66.
31. Liu Y, Lu Q, Xi L, Gong Y, Su J, Han D, Zhang Z, Liu H, Jin J, Yang Y. Effects of replacement of dietary fishmeal by cottonseed protein concentrate on growth performance, liver health, and intestinal histology of largemouth bass (*Micropterus salmoides*). Front Physiol. 2021;12:764987.
32. Kari ZA, Kabir MA, Mat K, Rusli ND, Razab MKAA, Ariff NSNA, Edinur HA, Rahim MZA, Pati S, Dawood MA. The possibility of replacing fish meal with fermented soy pulp on the growth performance, blood biochemistry, liver, and intestinal morphology of African catfish (*Clarias gariepinus*). Aquacult Rep. 2021;21:100815.
33. Xu Z, Regenstein JM, Xie D, Lu W, Ren X, Yuan J, Mao L. The oxidative stress and antioxidant responses of Litopenaeus vannamei to low temperature and air exposure. Fish Shellfish Immun. 2018;72:564–71.
34. Rastiannasab A, Afsharmanesh S, Rahimi R, Sharifian I. Alternations in the liver enzymatic activity of common carp, *Cyprinus carpio* in response to parasites, Dactylogyrus spp. and Gyrodactylus spp. J Parasitic Dis. 2016;40:1146–9.
35. Nazeri S, Farhangi M, Modarres S. The effect of different dietary inclusion levels of rutin (a flavonoid) on some liver enzyme activities and oxidative stress indices in rainbow trout, *Oncorhynchus mykiss* (Walbaum) exposed to Oxytetracycline. Aquac Res. 2017;48(8):4356–62.
36. Manneken JD, Dauer MVP, Currie PD. Dynamics of muscle growth and regeneration: lessons from the teleost. Exp Cell Res. 2022;411(2):112991.
37. Mohammadabadi M, Bordbar F, Jensen J, Du M, Guo W. Key genes regulating skeletal muscle development and growth in Farm animals. Animals. 2021;11(3):835.
38. Leduc-Gaudet JP, Hussain SN, Barreiro E, Gouspillou G. Mitochondrial dynamics and mitophagy in skeletal muscle health and aging. Int J Mol Sci. 2021;22(15):8179.
39. Ali A, Shaalan WM, Al-Tobasei R, Salem M. Coding and noncoding genes involved in atrophy and compensatory muscle growth in Nile Tilapia. Cells. 2022;11(16):2504.
40. Wrighton PJ, Shwartz A, Heo J-M, Quenzer ED, LaBella KA, Harper JW, Goessling W. Quantitative intravital imaging in zebrafish reveals in vivo dynamics of physiological-stress-induced mitophagy. J Cell Sci. 2021;134(4):jcs256255.
41. Yan X, Sun Q, Ji J, Zhu Y, Liu Z, Zhong Q. Reconstitution of leucine-mediated autophagy via the mTORC1-Barkor pathway in vitro. Autophagy. 2012;8(2):213–21.
42. He C. Balancing nutrient and energy demand and supply via autophagy. Curr Biol. 2022;32(12):R684–96.
43. Zhou Z, He Y, Wang S, Wang Y, Shan P, Li P. Autophagy regulation in teleost fish: a double-edged sword. Aquaculture. 2022;558:738369.
44. Hoseinifar SH, Yousefi S, Van D, Ashouri G, Gioacchini G, Maradonna F, Carnevali O. Oxidative stress and antioxidant defense in fish: the implications of probiotic, prebiotic, and synbiotics. Rev Fish Sci Aquac. 2020;29(2):198–217.
45. El AM, El RA, Edrise BM, Abdel MM, Jover M, Tomás A, Prince A, Davies SJ, Goda AS. Impact of nucleotide enriched diets on the production of gilthead seabream, *Sparus aurata* fingerlings by modulation of liver mitochondrial enzyme activitity, antioxidant status, immune gene expression, and gut microbial ecology. Aquaculture. 2021;535:736398.
46. Dam CTM, Ventura T, Booth M, Pirozzi I, Salini M, Smullen R, Elizur A. Intestinal transcriptome analysis highlights key differentially expressed genes involved in nutrient metabolism and digestion in yellowtail kingfish (*Seriola lalandi*) fed terrestrial animal and plant proteins. Genes. 2020;11(6):621.
47. Liu C, Zhao L, Shen Y. A systematic review of advances in intestinal microflora of fish. Fish Physiol Biochem. 2021:1–13.
48. Liu H, Dong X, Tan B, Du T, Zhang S, Yang Y, Chi S, Yang Q, Liu H. Effects of fish meal replacement by low-gossypol cottonseed meal on growth performance, digestive enzyme activity, intestine histology and inflammatory gene expression of silver sillago (*Sillago sihama* Forsskál)(1775). Aquacult Nutr. 2020;26(5):1724–35.
49. He M, Li X, Poolsawat L, Guo Z, Yao W, Zhang C, Leng X. Effects of fish meal replaced by fermented soybean meal on growth performance, intestinal histology and microbiota of largemouth bass (*Micropterus salmoides*). Aquacult Nutr. 2020;26(4):1058–71.
50. Song C, Liu B, Xu P, Xie J, Ge X, Zhou Q, Sun C, Zhang H, Shan F, Yang Z. Oxidized fish oil injury stress in Megalobrama amblycephala: evaluated by growth, intestinal physiology, and transcriptome-based PI3K-Akt/NF-κB/TCR inflammatory signaling. Fish Shellfish Immun. 2018;81:446–55.
51. Yamaguchi N, Knaut H. Focal adhesion-mediated cell anchoring and migration: from in vitro to in vivo. Development. 2022;149(10):dev200647.
52. Wang Y, Wang L, Zhang C, Song K. Effects of substituting fishmeal with soybean meal on growth performance and intestinal morphology in orange-spotted grouper (*Epinephelus coioides*). Aquacult Rep. 2017;5:52–7.
53. Amin A, El Asely A, Abd El-Naby AS, Samir F, El-Ashram A, Sudhakaran R, Dawood MA. Growth performance, intestinal histomorphology and growth-related gene expression in response to dietary Ziziphus mauritiana in Nile tilapia (*Oreochromis niloticus*). Aquaculture. 2019;512:734301.
54. Ganguly S, Dora KC, Sarkar S, Supratim C. Supplementation of prebiotics in fish feed: a review. Rev Fish Biol Fisheries. 2013;23:195–9.

55. Dawood MA. Nutritional immunity of fish intestines: important insights for sustainable aquaculture. Rev Aquacult. 2021;13(1):642–63.
56. Chen S, Zhou Y, Chen Y, Gu J. Fastp: an ultra-fast all-in-one FASTQ preprocessor. Bioinformatics. 2018;34(17):i884–90.
57. Bolger AM, Lohse M, Usadel B. Trimmomatic: a flexible trimmer for Illumina sequence data. Bioinformatics. 2014;30(15):2114–20.
58. Zhong Z, Fan J, Tian Y, Lin M, Zhu H, Ma D. Whole-genome resequencing and RNA-seq analysis implicates GPR75 as a potential genetic basis related to retarded growth in South China carp (*Cyprinus carpio rubrofuscus*). Genomics. 2024;116(5):110934.
59. Kim D, Langmead B, Salzberg SL. HISAT: a fast spliced aligner with low memory requirements. Nat Methods. 2015;12(4):357–60.
60. Pertea M, Kim D, Pertea GM, Leek JT, Salzberg SL. Transcript-level expression analysis of RNA-seq experiments with HISAT, StringTie and Ballgown. Nat Protoc. 2016;11(9):1650–67.
61. Love MI, Huber W, Anders S. Moderated estimation of Fold change and dispersion for RNA-seq data with DESeq2. Genome Biol. 2014;15(12):1–21.
62. Wu T, Hu E, Xu S, Chen M, Guo P, Dai Z, Feng T, Zhou L, Tang W, Zhan L. clusterProfiler 4.0: a universal enrichment tool for interpreting omics data. Innov. 2021;2(3):100141.

Publisher's note